Deletion of the pH Sensor GPR4 Decreases Renal Acid Excretion

Xuming Sun,*† Li V. Yang,‡ Brian C. Tiegs,§ Lois J. Arend,‖ Dennis W. McGraw,*† Raymond B. Penn,§ and Snezana Petrovic*†

*Department of Medicine, University of Cincinnati, Cincinnati, Ohio; †Research Services, Veterans' Affairs Medical Center, Cincinnati, Ohio; ‡Department of Medicine, East Carolina University, Greenville, North Carolina; ‖Department of Pathology, Johns Hopkins Hospital, Baltimore, Maryland; and §Department of Medicine, University of Maryland Baltimore, Baltimore, Maryland

ABSTRACT

Proton receptors are G protein-coupled receptors that accept protons as ligands and function as pH sensors. One of the proton receptors, GPR4, is relatively abundant in the kidney, but its potential role in acid-base homeostasis is unknown. In this study, we examined the distribution of GPR4 in the kidney, its function in kidney epithelial cells, and the effects of its deletion on acid-base homeostasis. We observed GPR4 expression in the kidney cortex, in the outer and inner medulla, in isolated kidney collecting ducts, and in cultured outer and inner medullary collecting duct cells (mOMCD1 and mIMCD3). Cultured mOMCD1 cells exhibited pH-dependent accumulation of intracellular cAMP, characteristic of GPR4 activation; GPR4 knockdown attenuated this accumulation. *In vivo*, deletion of GPR4 decreased net acid secretion by the kidney and resulted in a nongap metabolic acidosis, indicating that GPR4 is required to maintain acid-base homeostasis. Collectively, these findings suggest that GPR4 is a pH sensor with an important role in regulating acid secretion in the kidney collecting duct.

J Am Soc Nephrol 21: 1745–1755, 2010. doi: 10.1681/ASN.2009050477

Daily changes in the amount of protein in the diet produce fluctuations in metabolic net acid production. The kidneys adjust to these daily variations, ensuring tight correlation between acid production and excretion.[1,2] In humans, net acid excretion significantly correlates with changes in blood P_{CO2}, pH, and bicarbonate levels.[2] Physiologic changes of P_{CO2}, pH, and bicarbonate concentrations can therefore regulate net acid excretion, but this regulation is poorly understood.

The recently discovered family of "proton-activated" G protein-coupled receptors (GPCRs) represents candidate pH sensors capable of relaying information about local and/or systemic pH to acid-secreting cells in the kidney.[3–7] Several investigators have demonstrated that GPR4 (G protein-coupled receptor 4),[4,8,9] OGR1 (ovarian cancer G protein-coupled receptor 1, GPR68),[4,10–12] and TDAG8 (T cell death-associated gene 8, GPR65) can be stimulated by a reduction in extracellular pH to induce second messenger generation.[13–16] An elegant study by Ludwig *et al.*[4] demonstrated that mutation of specific putative proton-accepting histidine residues in OGR1 significantly impaired acid-stimulated phosphoinositide generation. *Ex vivo* studies from OGR1 knockouts indicate that OGR1 is the pH sensor, mediating the release of calcium from the bone during metabolic acidosis.[12] Analysis of aortic rings isolated from GPR4 knockout mice indicated that GPR4 acts as a pH sensor in blood vessels, regulating the outgrowth of new

Received May 5, 2009. Accepted June 12, 2010.

Published online ahead of print. Publication date available at www.jasn.org.

Correspondence: Dr. Snezana Petrovic, Division of Nephrology and Hypertension, Department of Medicine, ML0585, University of Cincinnati College of Medicine, 231 Albert Sabin Way, Cincinnati, OH 45267-0585. Phone: 513-861-3100, ext. 4441; Fax: 513-475-6415; E-mail: snezana.petrovic@uc.edu

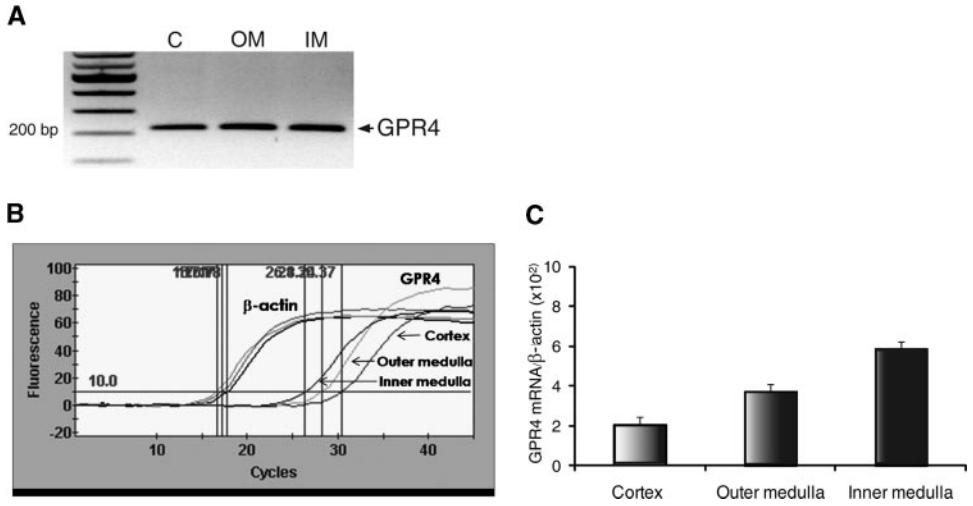

Figure 1. GPR4 mRNA is expressed in all three kidney zones with higher levels of expression in the medulla than in the cortex. (A) Representative gel image, demonstrating GPR4 real-time RT-PCR end products (218 bp) in the mouse kidney cortex, outer medulla, and inner medulla. (B) Corresponding real-time RT-PCR growth curves for GPR4 and β-actin mRNA in the kidney zones. (C) Ratios of GPR4 mRNA/β-actin mRNA in the three kidney zones. GPR4 mRNA expression in the mouse kidney is 1.8 times higher in the outer medulla and 2.9 times higher in the inner medulla than in the cortex.

capillaries in an acidic environment.[8] Of the three receptors, only GPR4 is relatively abundant in the kidney and overexpressed in solid kidney tumors,[15,17] but its function in the kidney has not been elucidated.

GPR4 has been speculated to function as a pH sensor in the kidney because it is expressed in the kidney at relatively high levels, activated in the physiologic pH range, and mediates the accumulation of intracellular cAMP, which is known to regulate the activity of acid-base transport proteins in the kidney collecting duct.[3–7,18] This study was designed to determine the role of GPR4 in acid-base regulation. We found that GPR4 mRNA was expressed in the kidney collecting duct, where GPR4 mediated accumulation of intracellular cAMP. Deletion of the GPR4 gene resulted in defective net acid excretion and was associated with a spontaneous nongap metabolic acidosis. On the basis of these studies, we propose that the proton receptor GPR4 functions as a pH sensor to regulate acid secretion by the collecting duct *in vivo*.

RESULTS

GPR4 Is Expressed in the Kidney Collecting Duct

Because pH-sensitive GPCR GPR4 is expressed at the highest level in the lung and kidney, the very two organs responsible for acid-base regulation,[17] we examined GPR4 mRNA distribution in the mouse kidney with real-time reverse transcription-polymerase chain reaction (RT-PCR) (a lack of useful antibodies precludes protein characterization). The data show that GPR4 mRNA was expressed in the kidney cortex, outer medulla, and inner medulla (Figure 1A) and that GPR4 mRNA expression was 1.8 times higher in the outer medulla and 2.9 times higher in the inner medulla than in the cortex (Figure 1, B and C). To further define GPR4 expression, we determined its distribution in nephron segments. We amplified GPR4 mRNA from isolated collecting ducts and detected some GPR4 mRNA expression in thick ascending limbs, but not in proximal tubules (Figure 2A). The results were verified by excision and sequencing of the RT-PCR products, and by the absence of RT-PCR products using RNA from GPR4$^{-/-}$ (Figure 2B).

We also examined cells cultured from mouse outer (mOMCD1) and inner (mIMCD3) medullary collecting ducts and found that mOMCD1 and mIMCD3 cells expressed GPR4 mRNA (Figure 3A). As is the case in tissue, GPR4 mRNA expression was higher in the inner than the outer medullary cells (Figure 3B).

We concluded that GPR4 mRNA is expressed in the kidney collecting duct, with low levels of expression in the thick ascending limbs of Henle. Both segments are actively involved in acid-base regulation.

Magnitude of pH-Dependent cAMP Response in mOMCD1 Cells Depends on the Level of GPR4 Expression

We wanted to ascertain whether cultured collecting duct cells, which express GPR4 endogenously, also accumulate cAMP upon change in extracellular pH. For these experiments we employed mOMCD1 cells, which although transformed, secrete acid, readily adapt to low pH,[19] and express H^+-ATPase and anion exchanger-1 (AE1), typical markers of A intercalated cells (Supplement 1, Figures S1 and S2).

Ludwig *et al.* demonstrated that human embryonic kidney (HEK-293) cells transfected with GPR4 exhibited higher baseline cAMP activity than nontransfected cells and accumulated cAMP in a pH-dependent manner.[4] Using the same protocol, we found that cAMP concentration in mOMCD1 also varied in

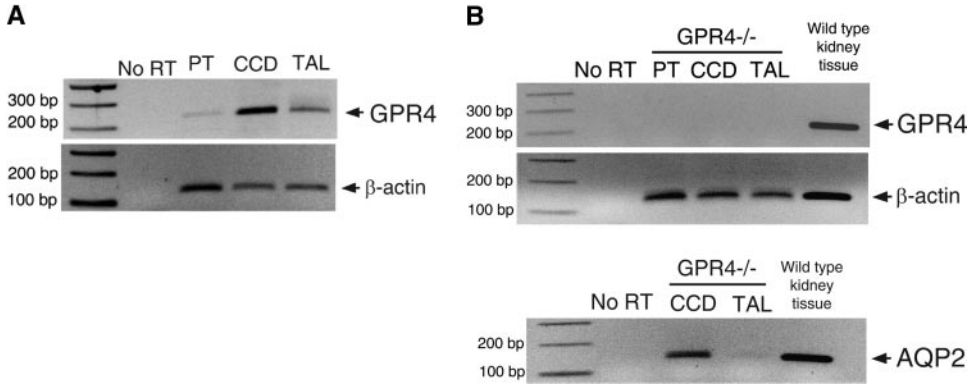

Figure 2. GPR4 mRNA is expressed in isolated collecting ducts. (A) Representative gel image of GPR4 RT-PCR products, which were abundant in CCD (cortical collecting duct), could be detected in TAL (thick ascending limb), and were virtually absent from PT (proximal tubule). The specificity of the bands was confirmed by sequencing. The lower panel shows β-actin expression. Unlike GPR4 mRNA, we could efficiently amplify β-actin from the proximal tubule. (B) GPR4 could not be amplified from the nephron segments isolated from GPR4 knockout mice (upper panel), whereas it was amplified from the wild-type kidney tissue (the far right line), which served as a positive control. In addition, we were able to amplify β-actin from all nephron segments (middle panel). The lower panel shows that we could also positively identify the collecting duct of GPR4 knockouts by amplifying a gene specific to the collecting duct (aquaporin 2-AQP2), from the collecting duct, but not from the thick ascending limb.

a pH-dependent manner (Figure 4B) with peak activity at 100 nM H^+ (pH 7.0). To ascertain that pH-dependent cAMP accumulation depended on GPR4 expression, we measured cAMP in mOMCD1 cells in which GPR4 expression was decreased with anti-GPR4 small interfering RNA (siRNA). Real-time RT-PCR analysis of the nontransfected mOMCD1 cells, mOMCD1 cells transfected with the control siRNA, which does not match any known sequence, and mOMCD1 cells transfected with anti-GPR4 siRNA demonstrated that anti-GPR4 siRNA decreased GPR4 mRNA expression approximately 50% (Figure 4A). Decreased GPR4 mRNA expression decreased pH-dependent cAMP activity approximately 50%. We repeated these experiments four times in different batches of mOMCD1 cells. Forskolin stimulation of cAMP production was not different among the nontransfected, control siRNA, and anti-GPR4 siRNA-transfected cells (not shown).

Because endogenous GPR4 protein levels cannot be quantified because of a lack of useful antibodies, we stably expressed a recombinant HA-tagged GPR4 in HEK-293 cells to assess the ability of GPR4 siRNA to knock down GPR4 protein and alter receptor-mediated cAMP accumulation in response to reduced media pH. As shown in Supplement 2, Supplemental Figure S3, HEK-293 cells stably expressing HA-GPR4 protein, but not vector transfected/selected cells, increased intracellular cAMP when stimulated with media ranging in pH from 8.0 to 6.0. Transient transfection of siRNA targeting GPR4, but not missense siRNA, reduced GPR4 protein levels by approximately 50% and reduced both baseline cAMP levels and accu-

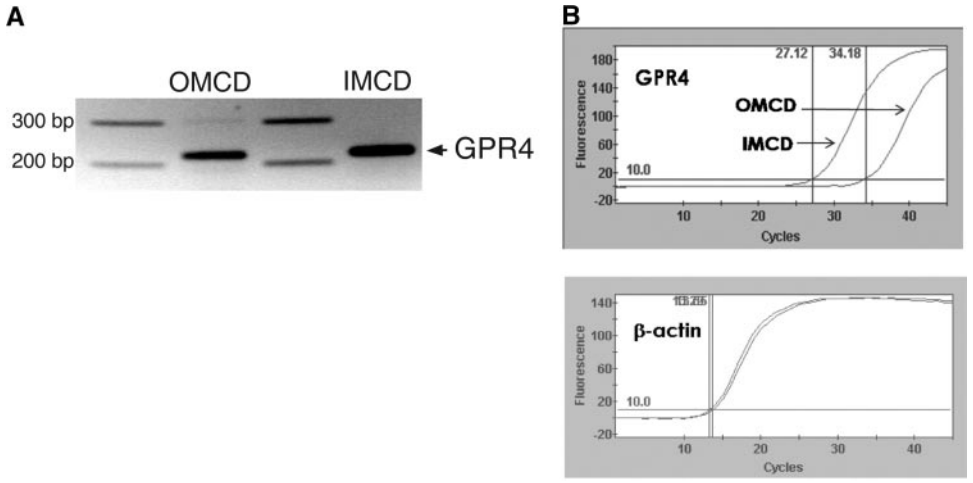

Figure 3. Cultured collecting duct cells derived from the mouse medulla exhibit abundant endogenous expression of GPR4. (A) GPR4 is detected as a 218-bp band in the mouse outer medullary (mOMCD1) and inner medullary (mIMCD3) collecting duct cell lines. (B) Corresponding real-time RT-PCR growth curves for GPR4 mRNA, illustrating the higher expression of GPR4 mRNA in mIMCD3 compared with mOMCD1 cells, similar to the mouse kidney tissue.

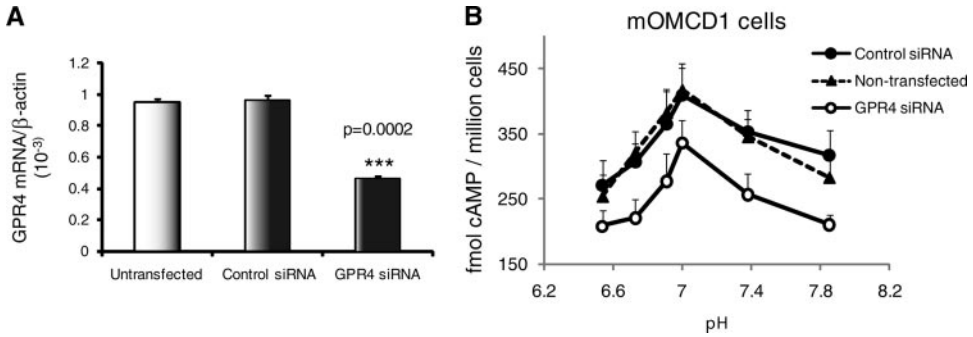

Figure 4. The magnitude of pH-dependent cAMP response in mOMCD1 cells decreases with a decreased level of GPR4 expression. Intracellular cAMP was measured by column chromatography in the presence of unspecific phosphodiesterase inhibitor IBMX in mOMCD1 cells exposed to buffers of different pH. To ensure that GPR4 mediated pH-dependent changes in intracellular cAMP concentration, we measured cAMP in nontransfected cells and cells transfected with control or anti-GPR4 siRNA. (A) Real-time RT-PCR analysis of nontransfected mOMCD1 cells and mOMCD1 cells transiently transfected with synthetic anti-GPR4 siRNA or with the control siRNA that does not match any known sequence. The analysis demonstrated that GPR4 expression decreased approximately 50% compared with mOMCD1 cells transfected with control siRNA or nontransfected cells. (B) mOMCD1 cells incubated in buffers of different pH accumulated cAMP in a pH-dependent manner (full triangles) and so did the cells transiently transfected with the control siRNA. Correlating well with the decreased GPR4 mRNA, pH-dependent accumulation of cAMP decreased in the cells transiently transfected with synthetic anti-GPR4 siRNA (empty circles). These experiments were done in four different batches of mOMCD1 cells.

mulation induced by lowering pH. These data were qualitatively similar to those generated for mOMCD1 cells depicted in Figure 4.

Deletion of GPR4 Results in Defective Acid Excretion by the Kidney

GPR4 knockout mice[8] ($GPR4^{-/-}$) were employed to assess the role of GPR4 in acid-base regulation. We analyzed arterial blood samples from nonanesthetized mice and found that $GPR4^{-/-}$ exhibit nongap metabolic acidosis (Table 1). At baseline, $GPR4^{-/-}$ had significantly lower blood bicarbonate (20.3 ± 0.6 mmol/L [$n = 20$]) than $GPR4^{+/+}$ (24 ± 0.4 mmol/L [$n = 15$]) ($P = 0.00001$). Because blood-gas analysis relies on calculated bicarbonate values, we confirmed these results by measuring bicarbonate directly using a spectrophotometric assay. Directly measured serum bicarbonate in $GPR4^{+/+}$ was 22.3 ± 0.38 ($n = 14$) *versus* 20.5 ± 0.62 ($n = 14$) in $GPR4^{-/-}$ ($P = 0.02$). Blood P_{CO2} was lower in $GPR4^{-/-}$, likely as a compensation for lower bicarbonate levels. $GPR4^{-/-}$ also had increased base excess and slightly higher blood chloride; therefore, the anion gap was in the normal range (Table 1).

Despite metabolic acidosis, urine pH was more alkaline in $GPR4^{-/-}$ (6.4 ± 0.06; $n = 20$) than in $GPR4^{+/+}$ (6.1 ± 0.04, $n = 15$, $P = 0.00003$). Higher urine pH in the face of metabolic acidosis suggested a defect in acid excretion. Therefore, we collected urine under oil in metabolic cages and determined net acid excretion (NAE) over a period of 24 hours. NAE was defined as the sum of urine ammonium and titratable acidity minus urine bicarbonate. Results indicated that higher urine pH in $GPR4^{-/-}$ was associated with reduced NAE (Table 1, Figure 5). The lower NAE in $GPR4^{-/-}$ did not result from the decreased GFR because there was no difference in creatinine clearance between $GPR4^{-/-}$ and $GPR4^{+/+}$, respectively (Table 1). We also examined multiple kidney sections in $GPR4^{-/-}$ and $GPR4^{+/+}$ with hematoxylin-eosin, periodic acid-Schiff, and trichrome staining and did not find evidence of pathologic changes in the kidney parenchyma (Supplement 3, Supplemental Figures S4, S5, and S6) nor a change in the number or size of glomeruli. We also performed the NGAL (neutrophil gelatinase-associated lipocalin) assay as a more sensitive measure of kidney injury,[20] but did not find a significant difference between $GPR4^{-/-}$ and $GPR4^{+/+}$ (data not shown).

We concluded that although $GPR4^{-/-}$ and $GPR4^{+/+}$ were at a steady state at baseline, $GPR4^{-/-}$ were spontaneously acidotic; that is, they exhibited a significantly lower plasma bicarbonate concentration, suggesting that the proton receptor GPR4 is involved in the maintenance of acid-base homeostasis.

Defective Response of GPR4 Knockout Mice to Acid Challenge

We next examined the response of $GPR4^{+/+}$ and $GPR4^{-/-}$ to acid challenge by addition of 280 mmol/L NH_4Cl in the drinking water for 4 days. On the fourth day, we measured electrolytes and NAE in the urine collected over 24 hours. Both $GPR4^{+/+}$ and $GPR4^{-/-}$ increased NAE after 4 days of acid loading, but the increase in NAE was blunted in $GPR4^{-/-}$ (Table 2, Figure 5). The titratable acidity component of NAE is comprised mainly of phosphate, so we measured urinary phosphate at baseline and during acid loading (Figure 6). The ratio of urinary phosphate (mmol/L) to creatinine (mmol/L) concentration was 12 ± 0.4 in $GPR4^{+/+}$ *versus* 10.2 ± 0.3 in $GPR4^{-/-}$; ($P = 0.01$, $n = 5$ of each) at baseline and 14.1 ± 0.6 in $GPR4^{+/+}$ *versus* 11.8 ± 0.5 in $GPR4^{-/-}$ ($P = 0.017$, $n = 5$ of each) after the first day of acid loading, but there was no significant difference in urine phosphate between $GPR4^{+/+}$ and $GPR4^{-/-}$ from the second to fourth day of acid loading. The lower NAE in $GPR4^{-/-}$ was not caused by decreased food or protein intake or a lower acid load as these parameters were

Table 1. Acid-base and electrolyte status of proton receptor knockout mice ($GPR4^{-/-}$) and their wild types ($GPR4^{+/+}$)

Genotype	$GPR4^{+/+}$	$GPR4^{-/-}$	*P*
Blood			
n	15	20	
pH	7.39 ± 0.01	7.37 ± 0.01	0.26
P_{CO2}	39.6 ± 0.9	35.7 ± 1.1[b]	0.006
P_{O2}	91.6 ± 4.4	92.2 ± 4.7	0.8
HCO_3^-	24 ± 0.4	20.3 ± 0.6[c]	0.00001
tCO_2	25.1 ± 0.4	21.7 ± 0.6[c]	0.00004
K^+	4.8 ± 0.07	5.3 ± 0.05[c]	0.0001
Na^+	146.3 ± 0.9	145.6 ± 1.1	0.6
Cl^-	116.3 ± 1	119.4 ± 0.6[a]	0.02
iCa^+	1.03 ± 0.06	1.05 ± 0.03	0.8
BEecf	−1.6 ± 0.5	−4.8 ± 0.7[c]	0.001
anion gap	11 ± 0.9	11.2 ± 0.6	0.5
creatinine	0.023 ± 0.002	0.025 ± 0.002	0.5
BUN	24 ± 1.1	26 ± 1.4	0.2
Urine			
pH	6.08 ± 0.04	6.37 ± 0.06[c]	0.00003
osmolarity	3057 ± 296	4220 ± 371[a]	0.04
creatinine	6.7 ± 0.6	7.9 ± 0.8	0.24
K^+/creatinine	55.3 ± 2.8	54.8 ± 2.9	0.9
Na^+/creatinine	24.3 ± 1.3	24.8 ± 1.5	0.8
Cl^-/creatinine	37.8 ± 1.9	37.7 ± 1.6	0.9
Ca^{2+}/creatinine	0.14 ± 0.004	0.13 ± 0.003	0.3
NH_4^+/creatinine	10.6 ± 0.8	8.9 ± 0.6	0.1
HCO_3^-/creatinine	0.17 ± 0.03	0.18 ± 0.04	0.95
TA/creatinine	12.2 ± 0.9	9.7 ± 0.5[a]	0.016
NAE/creatinine	22.6 ± 1.2	18.4 ± 0.7[b]	0.005
NAE	0.19 ± 0.02	0.14 ± 0.01[a]	0.04
creatinine clearance	0.29 ± 0.02	0.23 ± 0.03	0.1

Blood samples were obtained from the tail artery in conscious mice. Urine analyses were performed on samples collected in metabolic cages over 24-hour period. Urine pH and ammonium measurements were also repeated in fresh urine samples to avoid artifacts associated with the prolonged collection of urine in metabolic cages. Concentrations of electrolytes, anion gap, creatinine, and titratable acids (TA) were expressed in mmol/L, NAE was expressed in mmol/24 hours, ratios of urine electrolytes *versus* creatinine were expressed as mmol/L *versus* mmol/L, and BUN was expressed in mg/dl, creatinine clearance in ml/min, osmolarity in mOsmol/L, and P_{CO2} in mmHg.
[a] $P < 0.05$.
[b] $P < 0.01$.
[c] $P < 0.005$.

comparable in $GPR4^{-/-}$ and $GPR4^{+/+}$ (Supplement 4, Supplemental Figures S7 and S8).

The hypercalciuria (Table 2) associated with metabolic acidosis was significantly more pronounced in $GPR4^{-/-}$ than in $GPR4^{+/+}$ (Figure 7). Typically, an experimentally induced acid load is in part buffered by the release of calcium from the bone, which is accompanied by bicarbonate, carbonate, hydroxyl, and phosphate release.[21] It seems reasonable to assume, therefore, that alkali released from the bone prevented the development of a more profound acidosis in acid-loaded $GPR4^{-/-}$.[21] The release of calcium from the bone during metabolic acidosis is accompanied by decreased calcium reabsorption[22] and concomitant hypercalciuria so that serum calcium levels do not change (Table 2). We have not, however, found differences

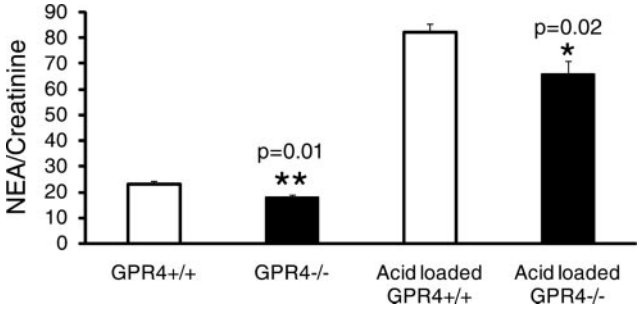

Figure 5. Proton receptor knockout mice ($GPR4^{-/-}$) exhibit decreased net acid excretion and attenuated response to acid challenge. GPR4 knockouts ($GPR4^{-/-}$) and their wild types ($GPR4^{+/+}$) were placed in metabolic cages and acid-loaded with NH_4Cl for 4 days. Net acid excretion was measured in the urine collected over 24 hours under oil. Both $GPR4^{+/+}$ and $GPR4^{-/-}$ increased acid secretion after acid challenge; however, this increase was blunted in $GPR4^{-/-}$. There were no differences in food, protein, water intake, and body weight between $GPR4^{-/-}$ and $GPR4^{+/+}$ during the experiment (Supplement 4).

in the expression of TRPV5 (transient receptor potential vanilloid channel type 5, which mediates decreased calcium reabsorption in the kidney during metabolic acidosis) protein between $GPR4^{-/-}$ and $GPR4^{+/+}$ (Supplement 6, Supplemental Figure S9), so further studies are needed to determine the pathophysiology of the exaggerated acid-induced hypercalciuria in $GPR4^{-/-}$.

Expression of OGR1 and TDAG8 in GPR4 Knockout Mice

To determine whether upregulation of other proton receptors could partially compensate for the deletion of GPR4, we measured OGR1 and TDAG8 gene expression in the kidneys of $GPR4^{-/-}$ and $GPR4^{+/+}$ by quantitative real-time RT-PCR and expressed the results as receptor/β-actin ratio. In $GPR4^{+/+}$, OGR1/β-actin ratio was $5.19 \times 10^{-5} \pm 0.7 \times 10^{-5}$ ($n = 5$) *versus* $4.9 \times 10^{-5} \pm 0.9 \times 10^{-5}$ ($n = 5$) in $GPR4^{-/-}$ ($P = 0.8$). TDAG8/β-actin ratio in $GPR4^{+/+}$ was $3.69 \times 10^{-4} \pm 0.4 \times 10^{-4}$ ($n = 5$) *versus* $3.44 \times 10^{-4} \pm 0.5 \times 10^{-4}$ ($n = 5$) in $GPR4^{-/-}$ ($P = 0.7$). Thus, OGR1 and TDAG8 mRNA expression, which was very low at baseline, did not change upon the deletion of GPR4. This does not however rule out the possibility that other pH-sensing mechanisms could be upregulated in $GPR4^{-/-}$ mice, alleviating the phenotype.

DISCUSSION

This study examined a pH-sensitive GPCR, the proton receptor GPR4, as a candidate pH sensor in the kidney.[3–7,18] We found that GPR4 mRNA is expressed in the kidney collecting duct, the nephron segment responsible for net acid excretion and final adjustments of the acid-base homeostasis. Cultured collecting duct cells (mOMCD1), which express GPR4 mRNA endogenously, exhibit pH-dependent accumulation of intra-

Table 2. Acid-base and electrolyte status of acid-loaded proton receptor knockout mice ($GPR4^{-/-}$) and their wild types ($GPR4^{+/+}$)

Genotype	$GPR4^{+/+}$	$GPR4^{-/-}$	*P*
Blood			
n	10	10	
pH	7.35 ± 0.02	7.32 ± 0.02	0.3
P_{CO2}	33 ± 1.7	34 ± 2.4	0.7
P_{O2}	96.5 ± 2	96.2 ± 4.6	0.9
HCO_3^-	18.3 ± 0.8	17.8 ± 0.5	0.6
tCO_2	19.3 ± 0.8	18.8 ± 0.5	0.7
K^+	5.3 ± 0.06	5.4 ± 0.1	0.4
Na^+	148.5 ± 1.7	150 ± 1.1	0.4
Cl^-	123 ± 4.5	133 ± 3.3	0.3
iCa^+	1.05 ± 0.06	1.1 ± 0.05	0.3
BEecf	−7.3 ± 1	−7 ± 0.4	0.7
creatinine[a]	0.018 ± 0.0007	0.018 ± 0.0002	0.6
BUN[a]	27 ± 3.3	29 ± 2	0.5
Urine			
n	5	5	
pH	5.85 ± 0.03	6.0 ± 0.07	0.2
osmolarity	4065 ± 152	2991 ± 442	0.051
creatinine	4.9 ± 0.1	5 ± 0.4	0.8
K^+/creatinine	65.5 ± 2.7	65.6 ± 1.3	0.9
Na^+/creatinine	31.4 ± 0.8	30.5 ± 1.6	0.6
Cl^-/creatinine	120.6 ± 3.5	117.6 ± 6.3	0.7
Ca^{2+}/creatinine	0.2 ± 0.01	0.3 ± 0.03[b]	0.02
NH_4^+/creatinine	62.6 ± 2	44.9 ± 4.4[c]	0.006
TA/creatinine	19.8 ± 2.5	21 ± 0.9	0.6
NAE/creatinine	82.3 ± 3.4	66 ± 5.1[b]	0.03
NAE	0.93 ± 0.03	0.66 ± 0.03[d]	0.0007
creatinine clearance	0.4 ± 0.02	0.4 ± 0.02	0.5

Blood samples were obtained from the tail artery in conscious mice.
[a]We used five wild types and five knockout animals for the measurements of blood creatinine and BUN. Urine analyses were performed on samples collected in metabolic cages during a 24-hour period. (Urine pH and ammonium measurements were also repeated in fresh urine samples to avoid artifacts associated with the prolonged collection of urine in metabolic cages.) Concentrations of electrolytes, anion gap, creatinine, and titratable acids (TA) were expressed in mmol/L, NAE was expressed in mmol/24 hours, ratios of urine electrolytes *versus* creatinine were expressed as mmol/L *versus* mmol/L, and BUN was expressed in mg/dl, creatinine clearance in ml/min, osmolarity in mOsmol/L, and P_{CO2} in mmHg. Acid-base and urine electrolyte parameters of wild-type mice at baseline were significantly different from the parameters measured in the acid-loaded wild types. Similarly, acid-base and electrolyte parameters of $GPR4^{-/-}$ mice at baseline were significantly different from the parameters of acid-loaded $GPR4^{-/-}$ mice (Supplement 5).
[b]$P < 0.05$.
[c]$P < 0.01$.
[d]$P < 0.005$.

cellular cAMP, characteristic of GPR4 activation. The deletion of the GPR4 gene resulted in a decrease in net acid excretion and spontaneous nongap metabolic acidosis, suggesting that the proton receptor GPR4 is required for maintenance of acid-base homeostasis.

The concept that the kidney uses a pH sensor to regulate acid excretion emerged from human and animal studies, demonstrating that net acid excretion tightly parallels fluctuations in acid load.[1,2] In healthy humans, differences in endogenous acid production account for 30%, and changes in P_{CO2} account for 40% of individual differences in plasma proton concentration.[2]

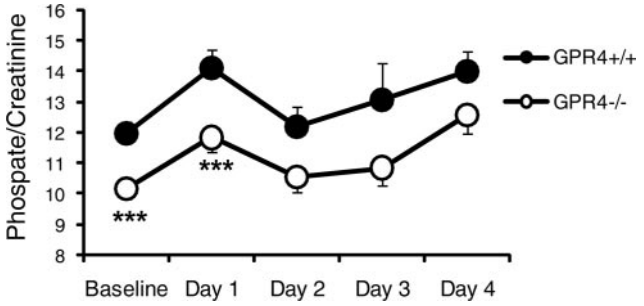

Figure 6. Proton receptor knockout mice ($GPR4^{-/-}$) have slightly lower urine phosphate compared to wild-type mice ($GPR4^{+/+}$) at baseline and after the first day of acid loading. Because urine titratable acidity primarily represents urine phosphate, we also measured phosphate in 24-hour urine samples collected from $GPR4^{-/-}$ and $GPR4^{+/+}$ in metabolic cages under oil before and during NH_4Cl loading.

Because the correlation between these variables and endogenous acid excretion is significant, it is plausible that these variables can regulate net acid excretion by the kidney. Accumulating evidence from *in vitro* and *ex vivo* studies indicates that kidney cells can sense changes in pH, bicarbonate, and P_{CO2}. Li *et al.* identified the adhesion kinase Pyk2 as a pH sensor that regulates the activity and expression of the sodium/proton exchanger NHE3, the acid-secreting transporter that mediates the bulk of bicarbonate reabsorption in the proximal tubule.[23] Zhou and Boron demonstrated that a basolateral P_{CO2} sensor, likely a tyrosine kinase, regulates bicarbonate reabsorption in perfused proximal tubules.[24] In sharks, gills are responsible for acid-base regulation. Gill epithelium expresses bicarbonate-activated soluble adenylyl cyclase (sAC) in a subset of base-secreting cells, and sAC activity appears to be essential for the maintenance of systemic bicarbonate levels with alkaline load *in vivo*.[25] Paunescu *et al.* demonstrated that H^+-

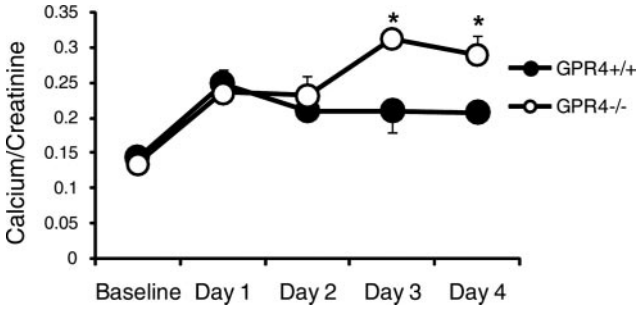

Figure 7. Increased urine calcium excretion in response to increased acid load is more pronounced in proton receptor knockout mice ($GPR4^{-/-}$) than the wild-type mice ($GPR^{+/+}$). Urine calcium was measured in 24-hour urine samples collected from $GPR4^{-/-}$ and $GPR4^{+/+}$ in metabolic cages under oil before and during NH_4Cl loading. Hypercalciuria elicited by acid loading was significantly more pronounced in $GPR4^{-/-}$ ($n = 5$) than in $GPR^{+/+}$ ($n = 5$) (*$P < 0.05$).

ATPase and bicarbonate-activated sAC associate physically in the intercalated cells (ICs) of the collecting duct.[26] The same group further demonstrated that cAMP stimulated apical H^+-ATPase accumulation and proton secretion in the collecting duct A-ICs *in vivo* and *in vitro*.[27] Our present investigation extends these findings by demonstrating that the activation of a pH-sensitive GPCR, GPR4, results in intracellular cAMP accumulation and is required for maintenance of acid-base balance by the kidney *in vivo*. Specifically, we show that at a balanced baseline state $GPR4^{-/-}$ exhibited significantly lower plasma bicarbonate concentration, lower net acid excretion, and higher urine pH than $GPR4^{+/+}$.

In the mammalian kidney, collecting ducts secrete net titratable acid,[28] so the defective net acid excretion in $GPR4^{-/-}$ is consistent with the expression and activity of GPR4 in the collecting duct. A preliminary report from Codina *et al.* indicated that, in the human kidney, GPR4 is localized to the basolateral membrane of the collecting duct A-ICs, suggesting a role for GPR4 in acid-base homeostasis in humans.[18]

Cultured collecting duct cells that express GPR4 mRNA endogenously exhibit peak GPR4 activity at pH 7.0, similar to findings in cells transfected with GPR4.[8,9,14,29] The dynamic range of (pH) responsiveness of GPR4 is consistent with a potential physiologic role for the receptor in the kidney interstitium. Although low pH of the kidney interstitium has been well appreciated,[30–32] a new technique allowed Andreev *et al.*[33] to demonstrate directly that fluctuations in interstitial pH were evident during changes in acid load. They used pHLIP (pH [low] insertion peptide) to show that under acid-secreting conditions in the kidney cortex and along the medullary rays, pH was at or below 7.0 (100 nM H^+), but shifted to more alkaline values (at or above 7.4) after bicarbonate loading. These data are consistent with Wesson's[32] studies, demonstrating that dietary acid load increases proton content of the renal cortex and increases NAE even in the absence of measurable change in plasma bicarbonate or pH. A proton receptor in the collecting duct should be positioned to function strategically as a sensor that can detect these changes and mediate adjustments in net acid excretion.

Activation of the proton receptor GPR4 results in the accumulation of intracellular cAMP, a second messenger well suited for mediating the adaptive response of acid-base transport proteins. Proton pumps, vacuolar H^+-ATPase and H^+-K^+-ATPase, and Cl^-/HCO_3^- exchangers, which mediate bicarbonate flux, are arranged in a polarized manner and used by acid- and bicarbonate-secreting intercalated cells (A-ICs and B-ICs, respectively) to balance acid and bicarbonate secretion. Cl^-/HCO_3^- exchangers in ICs are regulated by cAMP,[34] as are the proton pumps. The assembly of the subunits of H^+-ATPase is governed by cAMP in epithelial cells of the bowfly salivary gland.[35] In mouse A-ICs, cAMP stimulates apical V-ATPase accumulation and proton excretion *in vitro* and *in vivo*.[27] A study from Pastor-Soler and colleagues suggests that activity and subcellular localization of H^+-ATPase are coupled to the sensing of acid-base status via PKA.[36] The amino acid sequences of α-subunits of the H^+K^+-ATPase (HKα1 and HKα2) possess a consensus sequence for PKA-mediated phosphorylation. Rats treated by nonhydrolyzable analog of cAMP increased ouabaine-sensitive H^+K^+-ATPase acitivity (representing HKα2) in the cortical or medullary microsomes, an effect likely due to the insertion of HKα2 in the plasma membrane.[37] Codina *et al.* demonstrated that phosphorylation of S955 was necessary for full expression and functionality of HKα2[38] and that PKA contributed to HKα2 trafficking to the plasma membrane. Earlier studies from the DuBose' laboratory demonstrated that GPCRs are involved in the regulation of the kidney endosomal H^+-ATPase-mediated proton transport.[39] An accumulating body of evidence therefore indicates that cAMP and PKA play an important role in the regulation of the transport proteins that mediate proton and bicarbonate fluxes in the collecting ducts. A critical question is how this signaling pathway links to sensory mechanisms and whether it serves as a common final pathway that integrates the response to different sensors.

Despite metabolic acidosis present at a balanced steady state at baseline, $GPR4^{-/-}$ had more alkaline urine than did $GPR^{+/+}$ and exhibited a kidney acidification defect. These findings are similar to those of AE1 and Slc26a7 knockout mice, which lack a basolateral Cl^-/HCO_3^- exchanger in A-ICs[40,41] and are regarded as mouse models of distal renal tubular acidosis. However, the deletion of the B1 subunit of H^+-ATPase, a major acidification mechanism in the collecting duct, did not result in spontaneous metabolic acidosis.[42] Deletion of sodium/proton exchangers NHE3 and NHE3/NHE2 in the proximal tubule resulted only in mild acidosis.[43] The deletion of Rhcg, the ammonium transporter in the collecting duct, impairs ammonium secretion and response to an acid challenge, but does not render mice acidotic at baseline.[44,45] Therefore, the phenotype of $GPR4^{-/-}$ appears to be either similar or more pronounced than the phenotype of mouse models produced by the deletion of rate-limiting transport proteins involved in acid-base regulation.

In summary, this study demonstrates that the proton receptor GPR4 is involved in the regulation of acid-base balance *in vivo*, supporting the concept that a pH sensor may function to regulate kidney acid secretion appropriately. We anticipate that the proton receptor represents an important component of a sensory mechanism that integrates the response to changes in P_{CO2}, pH, and bicarbonate by the kidney. Additional studies will be needed to determine the precise mechanisms by which the proton receptor GPR4 functions to mediate regulation of acid secretion by the kidney collecting duct.

CONCISE METHODS

Animals

Black Swiss mice were purchased from Taconic (Germantown, NY). GPR4 knockout mice ($GPR4^{-/-}$)[8] were a gift from Owen Witte (University of California Los Angeles, Howard Hughes Med-

ical Institute, Los Angeles, California). GPR4 deletion and phenotype of $GPR4^{-/-}$ were previously described, and genotyping was done according to the published protocol.[8] The colony was established at the Animal Facility of the Veterans Affairs Medical Center in Cincinnati, Ohio. Only the procedures approved by the Institutional Animal Care and Use Committee of the VA Medical Center were used in this study. All animals ate standard laboratory mouse diet and drank tap water, except in the experiments in which mice were acid-loaded. The mice were euthanized with sodium pentobarbital and their kidneys harvested for expression and histochemical studies.

Acid-Base Status

Blood Samples and Blood Gas Analysis

Blood samples were obtained by a nick in tail artery in nonanesthetized mice. The samples were immediately injected into a blood gas analyzer IRMA TRUPOINT (International Technidyne Corp., Edison, NJ). We measured blood pH, P_{CO2}, bicarbonate, hematocrit, sodium, potassium, chloride, and ionized calcium, blood urea nitrogen (BUN), and creatinine. Because the blood gas analyzer calculates blood bicarbonate values based on P_{CO2} and blood pH measurements, and blood P_{CO2} measurement are prone to artifacts because animals might hyperventilate, we also measured serum bicarbonate directly with a spectrophotometric assay according to the manufacturer's protocol (Pointe Scientific, Inc., Canton, MI).

Urine Analyses

Urine samples were collected either as fresh samples or under oil for 24 hours in metabolic cages (Harvard Apparatus, Holliston, MA). In the metabolic cages, urine was collected after a 2-day adaptation period to the metabolic cage environment. Urine pH was measured with TWIN pH meter B-213 (Horiba Ltd., Kyoto, Japan). Sodium, potassium, and chloride were measured with indirect potentiometry using ion-specific electrodes. Urine osmolality was measured by freezing point–based osmometry (Advanced Instruments, Norwood, MA). The concentrations of the urine ammonium, calcium, phosphate, and bicarbonate were determined with spectrophotometric assays according to the manufacturer's protocol (Pointe Scientific, Inc.). Sulfate was measured with QuantiChrom Sulfate Assay Kit (BioAssay Systems, Hayward, CA). Titratable acidity was determined according to Chan *et al.*[46] Anion gap and net acid excretion were then calculated from the measured values.

Acid Loading

Acid loading was performed by adding 280 mM NH_4Cl plus 5% sucrose to drinking water for 4 days. The control group drank tap water. Addition of sucrose to NH_4Cl solution ensured comparable intake of fluid by control and acid-loaded animals (Supplement 4). Blood gas, electrolyte, and urine analyses were performed as described above. Particular attention was paid to food, water intake, and acid load, which within the 4-day period was not different between control and acid-loaded animals (Supplement 4, Supplemental Figure S7), nor was the intake of protein as suggested by lack of significant difference between wild types and knockouts in urine sulfate excretion (Supplement 4, Supplemental Figure S8).

RNA Isolation and RT-PCR

For the studies examining GPR4 distribution in the kidney, RNA was extracted from the kidney cortex, outer medulla, and inner medulla and dissected from the kidneys of Black Swiss mice. RNA was also extracted from the cultured outer and inner medullary collecting duct (mOMCD1 and mIMCD3) cells (cell origin and culture conditions are described below). For the expression studies looking at the expression of proton receptors other than GPR4, RNA was extracted from the kidneys of $GPR^{+/+}$ and $GPR4^{-/-}$.

Total cellular RNA was extracted with RNeasy Mini Kit (QIAGEN, Germantown, MD) according to the manufacturer's protocol. DNase I (QIAGEN, Hilden, Germany) was used to digest genomic DNA from the tissues during total RNA extraction and purification. Routinely, an RNA gel was run to assess purity and quality of the extracted total RNA. Quantitative analysis of total RNA was done with NanoDrop ND-1000 UV-vis spectrophotometer (NanoDrop Technologies, Wilmington, DE). One microgram of total RNA was reverse-transcribed to the first-strand cDNA with oligo $(dT)_{12\text{-}18}$ primer using SuperScrip First-Strand Synthesis System for RT-PCR (Invitrogen, Carlsbad, CA) according to the manufacturer's protocol. Real-time RT-PCR was run in triplicate for the quantitative analysis of mRNA expression levels and carried out using a 7500 Real-Time PCR System (Applied Biosystems, Foster City, CA) or a Smart Cycler System (Cepheid, CA). The primers for mouse β-actin, the proton receptors GPR4, OGR1, and TDAG8, were designed based on mRNA sequence of mouse β-actin (GenBank Accession Number: NM_007393), GPR4 (GenBank Accession Number: NM_175668), OGR1 (GenBank Accession Number: NM_175493), and TDAG8 (GenBank Accession Number: NM_008152). The primer sequences were as follows: β-actin: 5′-TTG CTG ACA GGA TGC AGA AG-3′ (sense), and 5′-CAG TGA GGC CAG GAT GGA GC-3′ (antisense); GPR4: 5′-CTA CCT GGC TGT GGC TCA T-3′ (sense), and 5′-CAA AGA CGC GGT ACA GAT TCA-3′ (antisense); OGR1: 5′-GGG TAT GGG GCT GGA TAG TT-3′ (sense), 5′-TAT TCC TCA TGG GCT TGG AG-3′ (antisense); TDAG8: 5′-GCA AGC GAA GAA GGA AAA TG-3′ (sense), 5′-GCA CAA GGT GGG AGA GAA AG-3′ (antisense). The size of PCR products for β-actin was 122 bp, 218 bp for GPR4, 231 bp for OGR1, and 139 bp for TDAG8. We routinely used β-actin as a control for sampling errors. Quantitative real-time RT-PCR reaction consisted of 1 μl of first-strand cDNA, 0.1 μM primers, 1× PCR buffer (without Mg^{2+}), 5.0 mM $MgCl_2$, 200 μM dNTP mix, 1 unit of Platinum Tag DNA polymerase (Invitrogen), and 0.25× SYBR Green I Nucleic Acid Gel Stain (Molecular Probes, Invitrogen, Eugene, OR) in a total volume of 25 μl. After an initial denaturation at 95°C for 10 minutes, 40 cycles of PCR were performed with denaturation at 95°C for 10 seconds, annealing at 64°C (β-actin, OGR1, TDAG8) or 66°C (GPR4) for 15 seconds, and extension at 72°C for 35 seconds. The absolute mRNA levels in each sample were calculated based on a standard curve. The standard curve was developed by using serial dilutions of known amounts of specific templates against corresponding cycle threshold values. To normalize gene expression, we then calculated the ratio of the gene over β-actin in each sample.[47,48] We verified the specificity of PCR

products for β-actin, GPR4, OGR1, and TDAG8 by examining the melting curve, electrophoresis, and sequencing of the real-time RT-PCR products.

Nephron Segment RT-PCR

RT-PCR using mRNA from isolated renal tubules was done according to our published protocols.[49] Proximal tubules, cortical thick ascending limbs, and cortical collecting ducts were hand-dissected from the kidneys of Black Swiss or GPR4 knockout mice at 4°C. The dissection solution consisted of 140 mM NaCl, 2.5 mM K_2HPO_4, 2 mM $CaCl_2$, 1.2 mM $MgSO_4$, 5.5 mM D-glucose, 1 mM sodium citrate, 4 mM sodium lactate, and 6 mM L-alanine, pH 7.4, and was bubbled with 100% O_2. The nephron segments were pooled and collected in the 0.5-ml tube with 50 μl of RNAlater RNA stabilization reagent (QIAGEN). After the samples were centrifuged at 13,000 rpm for 2 minutes at room temperature, RNAlater was removed and 8 μl of ice-cold tubule lysis solution was added. The lysis solution consisted of 0.9% Triton X-100, 5 mM dithiothreitol, and 1 U/μl RNaseOUT Recombinant RNase Inhibitor (Invitrogen). The tubules were reverse-transcribed using SuperScript First-Strand Synthesis System for RT-PCR (Invitrogen). A PCR reaction, which consisted of 2 μl of first-strand cDNA, 0.2 μM primers, 1× PCR buffer (without Mg^{2+}), 5.0 mM $MgCl_2$, 200 μM dNTP mix, and 2 units of Platinum Tag DNA polymerase (Invitrogen) in a total volume of 25 μl, was carried out by using a Mastercycler gradient (Eppendorf, Hamburg, Germany). After an initial denaturation at 95°C for 5 minutes, 45 cycles of PCR were performed with denaturation at 95°C for 30 seconds, annealing at 60°C for 30 seconds, and extension at 72°C for 1 minute. We used the same primers for both GPR4 and β-actin as described above. The primers for mouse aquaporin 2 (AQP2) were designed based on mRNA sequence of mouse aquaporin 2 (GenBank Accession Number NM_009699 and the primer sequences were as follows: 5′-TTG CCA TGT CTC CTT CCT TC-3′ (sense) and 5′-TTG TGG AGA GCA TTG ACA GC-3′ (antisense). The size of PCR products for AQP2 was 135 bp. Twenty microliter PCR products from each sample for GPR4 and β-actin were loaded on 1.2% agarose gel stained with ethidium bromide. The specificity of PCR products for GPR4, β-actin, and AQP2 was verified by sequencing.

Cell Culture

Human embryonic kidney 293 (HEK-293) cells (Life Technologies, Grand Island, NY), mouse outer medullary collecting duct (mOMCD1) cells (a gift from Dr. Thomas D. DuBose),[19] and inner medullary collecting duct (mIMCD3) cells[50] (a gift from Dr. Karl Matlin) were grown in DMEM with high glucose (Mediatech, Inc., Herndon, VA) at 37°C in an atmosphere of 5% CO_2. The media was supplemented with 5% FBS (Life Technologies, Grand Island, NY), 10 mM HEPES (Sigma, St. Louis, MO), pH 7.4, 2 mM L-glutamine (Sigma), and 100 U/ml of penicillin and 100 μg/ml of streptomycin (Life Technologies). Cell passages 10 to 20 were used for the experiments.

HEK-293 cells stably expressing HA-GPR4 were generated by transfection of cells with pcDNA3-HA-GPR4 using Fugene followed by selection with 250 μg/ml G418 (Supplement 2). Cells transfected with pcDNA3 vector and selected with G418 were generated as control cells.

cAMP Production

cAMP measurements in mOMCD1 cells were performed as published previously,[51] by using [^{3}H]-adenine and alumina column chromatography. The confluent cells grown in 24-well plates were loaded with [^{3}H]-adenine (2 μCi/ml per well) for 2 hours, then washed, and exposed to buffers of pH ranging from 6.5 to 7.8, or 100 μM forskolin in the presence of 1 mM of the phosphodiesterase inhibitor isobutylmethylxanthine (IBMX, Sigma) at 37°C for 15 minutes. We used a narrower pH range (6.6 to 7.8) than employed in the original report,[4] to better approximate the physiologic environment relevant to the function of the kidney. The buffers consisted of 130 mM NaCl, 0.9 mM NaH_2PO_4, 5.4 mM KCl, 0.8 mM $MgSO_4$, 1.0 mM $CaCl_2$, 25 mM glucose, 8 mM HEPES, 8 mM EPPS, and 8 mM MES. The pH of the buffer solutions was adjusted to various points ranging from 6.5 to 7.8. Effects of temperature on pH were carefully taken into account and the pH of all solutions was double-checked at 37°C after 15-minutes incubation. An unspecific phosphodiesterase inhibitor (IBMX, Sigma) was added at a final concentration of 1 mM, to allow cAMP accumulation without interference from phoshodiestereases. The reactions were terminated by the rapid addition of 100 μl of 2.2 M HCl. After the samples were frozen and thawed to ensure cell lysis, cAMP was eluted by alumina column chromatography. The [^{3}H]cAMP values were corrected for the adenine uptake, and column efficiency was ascertained with tracer [^{14}C]-cAMP. Each data point was determined and expressed as per million cells. All experiments were done in triplicate and repeated in four different batches of cells. Measurement of cAMP accumulation in HEK-293 cells heterologously expressing HA-GPR4 was performed as per Penn *et al.*[52]

siRNA

Four sets of synthetic siRNA molecules corresponding to the mouse GPR4 mRNA sequence (GenBank Accession No. NM_175668) and one set of negative control siRNA molecules, which do not correspond to any known gene (Silencer Cy 3-Labeled Negative Control), were purchased from Ambion (Austin, TX). The efficiency of the transfection was optimized with the control, fluorescently labeled siRNA. With use of the optimized conditions of transfection, the annealed siRNA molecules were transfected into mOMCD1 cells as Lipofectamine 2000 complexes in Opti-MEM I Reduced Serum Medium (Life Technologies) at a final concentration of 30 nM. After 48-hour incubation, total RNA was prepared from the transfected and mock-transfected cells, and GPR4 mRNA was analyzed by real-time RT-PCR. On average, we attained 52% knockdown of GPR4 mRNA. The most efficient GPR4 siRNA sequence was as follows, sense: 5′-GCA GGG CUG GUU UAG AAA G-3′, antisense: 5′-CUU UCU AAA CCA GCC CUG C-3′ (Ambion, Austin, TX). Nontransfected cells and cells transfected with either control or anti-GPR4 siRNA were used for cAMP measurements. HEK-293 cells stably transfected with pcDNA3 vector (Vector) or HA-GPR4 (GPR4) were plated on 60-mm dishes and transfected using Fugene with either 2.6 μg of either missense siRNA (CON) or siRNA targeting GPR4 (Dharmacon, Lafayette, CO) (Supplement 2, Supplemental Figure S3).

Statistical Analyses

Data are presented as mean ± SEM values. Comparisons were done using unpaired *t* test. $P < 0.05$ was considered statistically significant.

ACKNOWLEDGMENTS

Parts of this study were previously reported in preliminary form at the 2006 and 2008 annual meetings of the American Society of Nephrology (November 14 through 19, 2008, San Diego, CA, and November 4 through 9, 2008, Philadelphia, PA) and the Experimental Biology annual meeting (April 5 through 9, 2008, San Diego, CA). We are in debt to Dr. Robin Luke for many invaluable discussions and suggestions regarding this project. The authors thank Drs. Thomas DuBose, Prasad Devarajan, and Gary Shull for reading the manuscript and for their helpful suggestions. The technical assistance of Kari Brown with the column chromatography experiments is greatly appreciated. The authors are grateful for Dr. Rick Strait's help with blood sampling in nonanesthetized mice. We thank Drs. Qing Ma and Prasad Devarajan for NGAL assays and Dr. Cristina Furdui for the calculations of Kd values for GPR4 dose response in mOMCD1 cells. This work was supported by the Beginning Grant-in-Aid from the American Heart Association (0765363B), Paul Teschan Research Fund from Dialysis Clinic Inc., and Scientist Development Grant from the American Heart Association (0835313N) (to S.P.) and HL58506 (to R.B.P.).

DISCLOSURES

None.

REFERENCES

1. Gluck SL: Acid sensing in renal epithelial cells. *J Clin Invest* 114: 1696–1699, 2004
2. Kurtz I, Maher T, Hulter HN, Schambelan M, Sebastian A: Effect of diet on plasma acid-base composition in normal humans. *Kidney Int* 24: 670–680, 1983
3. Sun X, Petrovic S: Decreased net acid secretion in pH sensor knockout mice [Abstract]. *J Am Soc Nephrol* 19: 40A, 2008
4. Ludwig MG, Vanek M, Guerini D, Gasser JA, Jones CE, Junker U, Hofstetter H, Wolf RM, Seuwen K: Proton-sensing G-protein-coupled receptors. *Nature* 425: 93–98, 2003
5. Sun X, McGraw DW, Petrovic S: The proton-sensing receptor, GPR4, is a good candidate for an acid sensor in the kidney [Abstract]. *J Am Soc Nephrol* 17: 14A, 2006
6. Wagner CA, Kovacikova J, Stehberger PA, Winter C, Benabbas C, Mohebbi N: Renal acid-base transport: Old and new players. *Nephron Physiol* 103: 1–6, 2006
7. Brown D, Breton S, Ausiello DA, Marshansky V: Sensing, signaling and sorting events in kidney epithelial cell physiology. *Traffic* 10: 275–284, 2009
8. Yang LV, Radu CG, Roy M, Lee S, McLaughlin J, Teitell MA, Iruela-Arispe ML, Witte ON: Vascular abnormalities in mice deficient for the G protein-coupled receptor GPR4 that functions as a pH sensor. *Mol Cell Biol* 27: 1334–1347, 2007
9. Tobo M, Tomura H, Mogi C, Wang JQ, Liu JP, Komachi M, Damirin A, Kimura T, Murata N, Kurose H, Sato K, Okajima F: Previously postulated "ligand-independent" signaling of GPR4 is mediated through proton-sensing mechanisms. *Cell Signal* 19: 1745–1753, 2007
10. Tomura H, Wang JQ, Komachi M, Damirin A, Mogi C, Tobo M, Kon J, Misawa N, Sato K, Okajima F: Prostaglandin I(2) production and cAMP accumulation in response to acidic extracellular pH through OGR1 in human aortic smooth muscle cells. *J Biol Chem* 280: 34458–34464, 2005
11. Tomura H, Mogi C, Sato K, Okajima F: Proton-sensing and lysolipid-sensitive G-protein-coupled receptors: A novel type of multi-functional receptors. *Cell Signal* 17: 1466–1476, 2005
12. Frick KK, Krieger NS, Nehrke K, Bushinsky DA: Metabolic acidosis increases intracellular calcium in bone cells through activation of the proton receptor OGR1. *J Bone Miner Res* 24: 305–313, 2009
13. Ishii S, Kihara Y, Shimizu T: Identification of T cell death-associated gene 8 (TDAG8) as a novel acid sensing G-protein-coupled receptor. *J Biol Chem* 280: 9083–9087, 2005
14. Radu CG, Nijagal A, McLaughlin J, Wang L, Witte ON: Differential proton sensitivity of related G protein-coupled receptors T cell death-associated gene 8 and G2A expressed in immune cells. *Proc Natl Acad Sci U S A* 102: 1632–1637, 2005
15. Sin WC, Zhang Y, Zhong W, Adhikarakunnathu S, Powers S, Hoey T, An S, Yang J: G protein-coupled receptors GPR4 and TDAG8 are oncogenic and overexpressed in human cancers. *Oncogene* 23: 6299–6303, 2004
16. Wang JQ, Kon J, Mogi C, Tobo M, Damirin A, Sato K, Komachi M, Malchinkhuu E, Murata N, Kimura T, Kuwabara A, Wakamatsu K, Koizumi H, Uede T, Tsujimoto G, Kurose H, Sato T, Harada A, Misawa N, Tomura H, Okajima F: TDAG8 is a proton-sensing and psychosine-sensitive G-protein-coupled receptor. *J Biol Chem* 279: 45626–45633, 2004
17. Mahadevan MS, Baird S, Bailly JE, Shutler GG, Sabourin LA, Tsilfidis C, Neville CE, Narang M, Korneluk RG: Isolation of a novel G protein-coupled receptor (GPR4) localized to chromosome 19q13.3. *Genomics* 30: 84–88, 1995
18. Codina J, Du W, Willingham MC, Penn RB, DuBose TD Jr: GPR4 may serve as a pH sensor to regulate the colonic H^+,K^+-ATPase ($HKalpha_2$) in the renal medulla [Abstract]. *J Am Soc Nephrol* 19: 40A, 2008
19. Guntupalli J, Onuigbo M, Wall S, Alpern RJ, DuBose TD Jr.: Adaptation to low-K+ media increases H(+)-K(+)-ATPase but not H(+)-ATPase-mediated pHi recovery in OMCD1 cells. *Am J Physiol* 273: C558–C571, 1997
20. Devarajan P: NGAL in acute kidney injury: From serendipity to utility. *Am J Kidney Dis* 52: 395–399, 2008
21. Lemann J Jr, Bushinsky DA, Hamm LL: Bone buffering of acid and base in humans. *Am J Physiol Renal Physiol* 285: F811–F832, 2003
22. de Groot T, Bindels RJ, Hoenderop JG: TRPV5: An ingeniously controlled calcium channel. *Kidney Int* 74: 1241–1246, 2008
23. Li S, Sato S, Yang X, Preisig PA, Alpern RJ: Pyk2 activation is integral to acid stimulation of sodium/hydrogen exchanger 3. *J Clin Invest* 114: 1782–1789, 2004
24. Zhou Y, Boron WF: Role of endogenously secreted angiotensin II in the CO2-induced stimulation of HCO3 reabsorption by renal proximal tubules. *Am J Physiol Renal Physiol* 294: F245–F252, 2008
25. Tresguerres M, Parks SK, Salazar E, Levin LR, Goss GG, Buck J: Bicarbonate-sensing soluble adenylyl cyclase is an essential sensor for acid/base homeostasis. *Proc Natl Acad Sci U S A* 107: 442–447, 2010
26. Paunescu TG, Da Silva N, Russo LM, McKee M, Lu HA, Breton S, Brown D: Association of soluble adenylyl cyclase with the V-ATPase in renal epithelial cells. *Am J Physiol Renal Physiol* 294: F130–F138, 2008
27. Paunescu TG, Ljubojevic M, Russo LM, Winter C, McLaughlin MM, Wagner CA, Breton S, Brown D: cAMP stimulates apical V-ATPase accumulation, microvillar elongation, and proton extrusion in kidney collecting duct A-intercalated cells. *Am J Physiol Renal Physiol* 298: F643–F654, 2010
28. Hamm LL, Alpern RJ: Cellular mechanisms of renal tubular acidification. *The Kidney: Physiology and Pathophysiology*, edited by Seldin DW, Giebisch G, Philadelphia, Lippincott Williams & Wilkins, 2000, pp 1935–1979

29. Seuwen K, Ludwig MG, Wolf RM: Receptors for protons or lipid messengers or both? *J Recept Signal Transduct Res* 26: 599–610, 2006
30. DuBose TD Jr, Pucacco LR, Seldin DW, Carter NW: Direct determination of PCO2 in the rat renal cortex. *J Clin Invest* 62: 338–348, 1978
31. DuBose TD Jr, Pucacco LR, Lucci MS, Carter NW: Micropuncture determination of pH, PCO2, and total CO2 concentration in accessible structures of the rat renal cortex. *J Clin Invest* 64: 476–482, 1979
32. Wesson DE: Dietary acid increases blood and renal cortical acid content in rats. *Am J Physiol Renal Physiol* 274: 97–103, 1998
33. Andreev OA, Dupuy AD, Segala M, Sandugu S, Serra DA, Chichester CO, Engelman DM, Reshetnyak YK: Mechanism and uses of a membrane peptide that targets tumors and other acidic tissues in vivo. *Proc Natl Acad Sci U S A* 104: 7893–7898, 2007
34. Schuster VL: Function and regulation of collecting duct intercalated cells. *Annu Rev Physiol* 55: 267–288, 1993
35. Dames P, Zimmermann B, Schmidt R, Rein J, Voss M, Schewe B, Walz B, Baumann O: cAMP regulates plasma membrane vacuolar-type H+-ATPase assembly and activity in blowfly salivary glands. *Proc Natl Acad Sci U S A* 103: 3926–3931, 2006
36. Gong F, Alzamora R, Smolak C, Li H, Naveed S, Neumann D, Hallows KR, Pastor-Soler NM: Vacuolar H^+-ATPase apical accumulation in kidney intercalated cells is regulated by PKA and AMP-activated protein kinase. *Am J Physiol Renal Physiol* 298: F1162–F1169, 2010
37. Beltowski J, Marciniak A, Wojcicka G, Gorny D: Regulation of renal Na(+), K(+)-ATPase and ouabain-sensitive H(+), K(+)-ATPase by the cyclic AMP-protein kinase A signal transduction pathway. *Acta Biochim Pol* 50: 103–114, 2003
38. Codina J, Liu J, Bleyer AJ, Penn RB, DuBose TD Jr.: Phosphorylation of S955 at the protein kinase A consensus promotes maturation of the alpha subunit of the colonic H^+,K^+ -ATPase. *J Am Soc Nephrol* 17: 1833–1840, 2006
39. Gurich RW, Codina J, DuBose TD Jr.: A potential role for guanine nucleotide-binding protein in the regulation of endosomal proton transport. *J Clin Invest* 87: 1547–1552, 1991
40. Stehberger PA, Shmukler BE, Stuart-Tilley AK, Peters LL, Alper SL, Wagner CA: Distal renal tubular acidosis in mice lacking the AE1 (band3) Cl^-/HCO_3^- exchanger (slc4a1). *J Am Soc Nephrol* 18: 1408–1418, 2007
41. Xu J, Song P, Nakamura S, Miller M, Barone S, Alper SL, Riederer B, Bonhagen J, Arend LJ, Amlal H, Seidler U, Soleimani M: Deletion of the chloride transporter slc26a7 causes distal renal tubular acidosis and impairs gastric acid secretion. *J Biol Chem* 284: 29470–29479, 2009
42. Finberg KE, Wagner CA, Bailey MA, Paunescu TG, Breton S, Brown D, Giebisch G, Geibel JP, Lifton RP: The B1-subunit of the H(+) ATPase is required for maximal urinary acidification. *Proc Natl Acad Sci U S A* 102: 13616–13621, 2005
43. Ledoussal C, Woo AL, Miller ML, Shull GE: Loss of the NHE2 Na(+)/H(+) exchanger has no apparent effect on diarrheal state of NHE3-deficient mice. *Am J Physiol Gastrointest Liver Physiol* 281: G1385–G1396, 2001
44. Lee HW, Verlander JW, Bishop JM, Igarashi P, Handlogten ME, Weiner ID: Collecting duct-specific RhC glycoprotein deletion alters basal and acidosis-stimulated renal ammonia excretion. *Am J Physiol Renal Physiol* 296: F1364–F1375, 2009
45. Biver S, Belge H, Bourgeois S, Van Vooren P, Nowik M, Scohy S, Houillier P, Szpirer J, Szpirer C, Wagner CA, Devuyst O, Marini AM: A role for rhesus factor rhcg in renal ammonium excretion and male fertility. *Nature* 456: 339–343, 2008
46. Chan JC: The rapid determination of urinary titratable acid and ammonium and evaluation of freezing as a method of preservation. *Clin Biochem* 5: 94–98, 1972
47. Sun X, Petrovic S: Increased acid load and deletion of AE1 increase Slc26a7 expression. *Nephron Physiol* 109: 29–35, 2008
48. Sun X, Soleimani M, Petrovic S: Decreased expression of Slc26a4 (pendrin) and Slc26a7 in the kidneys of carbonic anhydrase II-deficient mice. *Cell Physiol Biochem* 21: 95–108, 2008
49. Petrovic S, Wang Z, Ma L, Soleimani M: Regulation of the apical Cl^-/HCO_3^- exchanger pendrin in rat cortical collecting duct in metabolic acidosis. *Am J Physiol Renal Physiol* 284: F103–F112, 2003
50. Cohen DM, Chin WW, Gullans SR: Hyperosmotic urea increases transcription and synthesis of egr-1 in murine inner medullary collecting duct (mIMCD3) cells. *J Biol Chem* 269: 25865–25870, 1994
51. McGraw DW, Mihlbachler KA, Schwarb MR, Rahman FF, Small KM, Almoosa KF, Liggett SB: Airway smooth muscle prostaglandin-EP1 receptors directly modulate beta2-adrenergic receptors within a unique heterodimeric complex. *J Clin Invest* 116: 1400–1409, 2006
52. Penn RB, Pascual RM, Kim YM, Krymskaya VP, Panettieri RA Jr., Benovic JL: Arrestin specificity for GPCRs in human airway smooth muscle. *J Biol Chem* 276: 32648–32656, 2001

Supplemental information for this article is available online at http://www.jasn.org/.